

Article

# Simultaneous Removal of Seven Pharmaceutical Compounds from a Water Mixture Using Modified Chitosan Adsorbent Materials

Myrsini Papageorgiou <sup>1</sup>, Konstantinos N. Maroulas <sup>2</sup>, Eleni Evgenidou <sup>1,3</sup>, Dimitrios N. Bikiaris <sup>4</sup>, George Z. Kyzas <sup>2</sup> and Dimitra A. Lambropoulou <sup>1,3,\*</sup>

- <sup>1</sup> Laboratory of Environmental Pollution Control, Department of Chemistry, Aristotle University of Thessaloniki, GR-541 24 Thessaloniki, Greece; evgenido@chem.auth.gr (E.E.)
- <sup>2</sup> Hephaestus Laboratory, Department of Chemistry, School of Science, Democritus University of Thrace, GR-654 04 Kavala, Greece
- <sup>3</sup> Center for Interdisciplinary Research and Innovation (CIRI-AUTH), Balkan Center, 10th km Thessaloniki-Thermi Rd, GR-570 01 Thessaloniki, Greece
- <sup>4</sup> Laboratory of Polymers, Department of Chemistry, Aristotle University of Thessaloniki, GR-541 24 Thessaloniki, Greece
- \* Correspondence: dlambro@chem.auth.gr; Tel.: +30-2310-997687; Fax: +30-2310-997859

**Abstract:** Pharmaceuticals are used to improve the lives of people across the globe. The high demand for their fabrication and use causes a very serious environmental threat since their presence is ubiquitous in aqueous matrices. For this reason, the synthesis, characterisation, and efficiency of three chitosan-based materials to eliminate pharmaceutical mixtures from aqueous solutions were examined in the present study. The target mixture comprised seven widely used drugs: carbamazepine, cyclophosphamide, adefovir, levofloxacin, metronidazole, glibenclamide, and trimethoprim. The grafting of poly(ethylene imine) and poly(acrylamide) on the chitosan structure allowed its physical characteristics to be controlled. An adsorption assessment was performed at different pH values, and it was concluded that pH = 4 was the optimum value. The adsorption kinetics revealed that the adsorption of a drug mixture involves a combination of physical and chemical adsorption. The adsorption process appeared to be finished after 1 h for all compounds of the studied mixture, with CS-AMI exhibiting the fastest kinetics. Mass adsorption experiments were also carried out to determine its effects. Overall, the grafting process significantly increased the adsorption capacity over the pristine material. Specifically, the highest capacity increase for CS-PEI was ~220% for carbamazepine, and for CS-AMI, it was 158% for trimethoprim. FT-IR, SEM, and XRD were used for the characterisation of the polymers. Based on the findings, the three materials are suggested as very effective adsorbents for the elimination of medicine residues from aqueous matrices.

**Keywords:** chitosan; modification; pharmaceutical mixture; adsorption; pollutants



**Citation:** Papageorgiou, M.; Maroulas, K.N.; Evgenidou, E.; Bikiaris, D.N.; Kyzas, G.Z.; Lambropoulou, D.A. Simultaneous Removal of Seven Pharmaceutical Compounds from a Water Mixture Using Modified Chitosan Adsorbent Materials. *Macromol* **2024**, *4*, 304–319. <https://doi.org/10.3390/macromol4020018>

Academic Editor: Ana María Díez-Pascual

Received: 1 April 2024

Revised: 4 May 2024

Accepted: 8 May 2024

Published: 11 May 2024



**Copyright:** © 2024 by the authors. Licensee MDPI, Basel, Switzerland. This article is an open access article distributed under the terms and conditions of the Creative Commons Attribution (CC BY) license (<https://creativecommons.org/licenses/by/4.0/>).

## 1. Introduction

Population increases and advancements in healthcare technology are responsible for the rising levels of pharmaceutical drug manufacturing and utilisation. However, unprocessed hospital and pharmaceutical industry effluents and inadequate medication waste management have led to the release of medicines into the environment. Specifically, pharmaceutical residues are persistent pollutants that pose a significant risk to human health even at tolerable concentrations since they are highly poisonous and have low biodegradable substances [1]. The presence of the active pharmaceutical components in multiple bodies of water was confirmed, with concentrations reaching around 100 ng/L in some cases and a little less than 50 ng/L in others. So far, the release of such pollutants into the environment has been unavoidable, posing an immense toxicity threat to ecosystems [2].

A broad spectrum of medicines has been identified in the environment, with studies indicating that nonsteroidal anti-inflammatory medications, psychiatric drugs, hormones, antibiotics, and other substances are frequently found in aquatic ecosystems [3,4]. They are partially metabolised after digestion, with metabolised and non-metabolised amounts being expelled from a living body [5]. As a result of insufficient metabolism, pharmaceuticals pass through urine and faeces into urban effluents [6]. Thus, thanks to the discharge of domestic, agricultural, hospital, and industrial wastes, traces of them can be observed in soil, groundwater, and surface water.

Despite the fact that these medications normally pass strict safety evaluations at conventional dosage thresholds, their accumulating remnants in the natural world have been related to behavioural abnormalities and endocrine disruption in some aquatic creatures [7]. Furthermore, pharmaceutical residues, particularly antibiotics, have been linked to the growth of antibiotic-resistant bacteria [8].

Several studies on environmental and pollution research have recently addressed this issue [1,9,10]. Consequently, the requirement to develop an effective removal process prompted a detailed examination of the current removal methods. Some of the most commonly used are (i) nanofiltration, (ii) electrolysis, (iii) reverse osmosis, (iv) ion exchange, (v) chemical disinfectants, and (vi) oxidation [11,12]. The drawbacks of the latter are their high-cost and the harmful effects of chemicals on the environment [13]. In contrast, adsorption is preferred for the remediation of pharmaceuticals and other pollutants because it provides numerous advantages, including cost-effectiveness, with an extensive selection of adsorbents, easy use, reusability, non-toxicity, and high effectiveness [14]. Adsorbents interact with pollutants via numerous interaction forces that occur via chemisorption or physisorption methods, including strong or weak chemical bonding or an exchange of electrons or transferring [15]. Materials that are commonly employed are activated carbon, carbon nanotubes, zeolites, and biochar [16].

The application of polymers, such as chitosan in solid phase extraction, produced promising results for the adsorption and preconcentration of these aqueous wastes [17]. Chitosan (poly- $\beta$ -(1 $\rightarrow$ 4)-2-amino-2-deoxy-D-glucose) is considered to be one of the most abundant natural biopolymers, created as the deacetylated derivative of chitin (from crustacean shells). Chitosan has been found to be a very effective adsorbent, commonly employed for the extraction of dyes [18] and other pollutants like heavy metals from wastewaters [19]. Chitosan's biocompatibility, high levels of biodegradability, and lack of toxicity characterise it as an environmentally friendly material. In addition, modified chitosan (grafted with various groups) was successfully employed as an adsorbent for pharmaceuticals such as pramipexole [20].

Although pharmaceutical adsorption has been investigated using various adsorbents, the simultaneous removal of pharmaceuticals with different physicochemical characteristics by adsorption on biopolymers such as chitosan remains a research challenge. The purpose of this study was to undertake in-depth research on the adsorption of pharmaceuticals with diverse functional groups in a multi-contaminant system. For the purposes of this work, chitosan was utilised for the elimination of a pharmaceutical mixture from water systems. Chitosan has hydroxyl groups in its matrix, which make it easy to be modified. In order to increase the adsorption efficiency of chitosan, poly(ethylene imine) (PEI) and poly(acrylamide) (AMI) were grafted so as to provide extra amino and imino units. This procedure was commonly used by other researchers [21,22]. The latter samples were then cross-linked with glutaraldehyde (GLA). The major novelty of this work is the simultaneous removal of pharmaceuticals along with the prepared materials, which has not been achieved in the past. In wastewaters, various pharmaceuticals exist simultaneously. The latter is not widely examined in research articles, but rather in single-component studies [23]. The objectives were (i) to evaluate the effect of various parameters, like temperature, pH, or the initial concentration of the drugs that may affect the process and (ii) to conduct kinetic and dosage experiments in order to achieve an integrated evaluation of the performance of the synthesised polymeric sorbent.

## 2. Materials and Methods

### 2.1. Materials

High-molecular-weight chitosan was obtained from Sigma-Aldrich (Darmstadt, Germany) and purified by extraction with acetone in a Soxhlet apparatus for 24 h, followed by drying under a vacuum at room temperature (25 °C). The average molecular weight was estimated at 3.55–105 g/mol, and the degree of deacetylation was 82 wt% [24,25]. Acrylamide (97% p.a.), isopropyl alcohol (99.7%), glutaraldehyde (50 wt% in water), and epichlorohydrin (99%) were obtained from Sigma-Aldrich. Poly(ethylene imine) (50% w/v in water) and sodium tripolyphosphate (98%) were obtained from Fluka (Buchs, Switzerland). Potassium persulfate (initiator) and dimethylformamide were obtained from Merck (Darmstadt, Germany). All solvents were of analytical grade.

### 2.2. Synthesis of Adsorbents

#### 2.2.1. Acrylamido-Modified Chitosan Derivative (CS-AMI)

For the preparation of the grafted chitosan with poly(acrylamide) (CS-AMI), an exact amount of chitosan (CS,  $2.25 \times 10^{-6}$  moles) was initially dissolved in a 2 v/v% acetic acid aqueous solution, followed by the addition of a solution of the monomer (AMI,  $3.38 \times 10^{-2}$  moles). This was followed by the addition of a solution of the initiator (KPS,  $5 \times 10^{-4}$  moles). The final solution (50 mL) was poured into a 100 mL stoppered flask, which was then placed in a thermostated bath at the desired reaction temperature (333 K) for 45 min. Prior to and during the polymerisation reaction, the solution was purged with argon. After the completion of the grafting reaction, the polymerisation mixture was rapidly cooled down to ambient temperature and neutralised to pH 8 with the addition of a 1 N NaOH solution. While stirring, the gel was poured into a large amount of acetone. After 24 h, satisfactory dewatering was achieved, and the hardened gel particles were filtered and exhaustively extracted with a methanol/water (7:3) solution in order to remove the unreacted monomer, the initiator and its by-products, and the poly(acrylamide) (PAMI) homopolymer that could eventually be formed during the grafting reaction. The dried remaining product at 323 K was considered the grafted copolymer.

#### 2.2.2. Poly(ethylene imine)-Modified Chitosan Derivative (CS-PEI)

Chitosan powder (CS-PEI) that was cross-linked and grafted with poly(ethylene imine) was prepared using the method in published studies in the literature [25–27]. Cross-linked chitosan powder suspended in water (total volume was 500 mL) was washed with 500 mL of isopropyl alcohol four times and then finally suspended in 500 mL of isopropyl alcohol. A total of 8.5 g of epichlorohydrin was added to the suspension. The amount of epichlorohydrin was equivalent to 3 times the amount of moles per glucosamine residue of chitosan. The reaction was carried out at 50 °C for 2 h. Thereafter, 100 mL of chitosan was well mixed in 100 mL of 30% poly(ethylene imine) aqueous solution at 80 °C for 3 h. The final product was washed with water thoroughly.

The final grafting percentages were determined on the basis of the percentage weight increase of the final product relative to the initial weight of chitosan,  $GP\% = 100\% \times (W_2 - W_1)/W_1$  ( $W_1$  and  $W_2$  denote the weight of chitosan before and after the grafting reaction, respectively). So, the GP% was as follows: CS-AMI, 40%; and CS-PEI, 45%.

### 2.3. Model Drug Pollutants

Seven pharmaceuticals were selected as target compounds in this research, namely carbamazepine, cyclophosphamide, adefovir, levofloxacin, metronidazole, glibenclamide, and trimethoprim, and they were all purchased from Aldrich (Darmstadt, Germany). These pharmaceuticals were selected because they are either widely used and detected or are resilient during treatment processes in an aqueous environment. Moreover, they have been evaluated to possess high environmental risk [28–32]. The list of studied pharmaceuticals, together with their pKa and pKow values, is shown in Table 1.

**Table 1.** Molecular formula and physicochemical properties of pharmaceuticals.

Name	M.F.	pKa	pKow	Solubility (mg/L)
Carbamazepine	C <sub>15</sub> H <sub>12</sub> N <sub>2</sub> O	13.9	2.45	17.7
Cyclophosphamide	C <sub>7</sub> H <sub>15</sub> Cl <sub>2</sub> N <sub>2</sub> O <sub>2</sub> P	5.7	0.63	40,000
Adefovir	C <sub>20</sub> H <sub>32</sub> N <sub>5</sub> O <sub>8</sub> P	2/6.8	1.91	19
Levofloxacin	C <sub>18</sub> H <sub>20</sub> FN <sub>3</sub> O <sub>4</sub>	6.24	−0.39/2.1	25
Metronidazole	C <sub>6</sub> H <sub>9</sub> N <sub>3</sub> O <sub>3</sub>	2.5	−0.02	9500
Glibenclamide	C <sub>23</sub> H <sub>28</sub> ClN <sub>3</sub> O <sub>5</sub> S	5.3	4.7	4
Trimethoprim	C <sub>14</sub> H <sub>18</sub> N <sub>4</sub> O <sub>3</sub>	6.6/7.2	1.33/0.91	400

## 2.4. Physicochemical Characterisation

### 2.4.1. SEM

The morphology of the prepared nanocomposites before and after enzymatic hydrolysis was examined using a JEOL JMS-840A (JEOL, Tokyo, Japan) scanning electron microscope (SEM) equipped with an energy-dispersive X-ray Oxford ISIS 300 microanalytical system (Oxford Instruments, Tubney Woods Abingdon, Oxfordshire, UK). All samples were coated with carbon black to avoid charging under the electron beam.

### 2.4.2. FTIR

Fourier-transform infrared spectroscopy (FTIR) spectra of all the samples were obtained using a Perkin-Elmer FTIR spectrophotometer, Spectrum One model, with the use of KBr disks (PerkinElmer, Waltham, MA, USA). The IR spectra of these films were obtained in absorbance mode and in the spectral region of 400–4.000 cm<sup>−1</sup> using a resolution of 4 cm<sup>−1</sup> and 64 co-added scans.

### 2.4.3. XRD

The patterns of XRD were taken using a Rigaku MiniFlex II (Rigaku Corporation, Tokyo, Japan) diffractometer with Bragg–Brentano geometry ( $\theta$ ,  $2\theta$ ) and Ni-filtered CuK $\alpha$  radiation. Analysis was performed on the synthesised chitosans. The samples were scanned over the internal range of 5–60° with a step of 0.05° and a rate of 1° min<sup>−1</sup>.

### 2.4.4. Swelling Tests

For the swelling tests, 1g of each one of the adsorbents was mixed with deionised water and left for a day to swell. Five consecutive measurements were required until the material was deemed fully swollen, i.e., the weight remained stable. Thereafter, filters were employed to isolate it from water, and filter paper was used to adsorb and remove the excess water. The swollen samples were measured, and the level of swelling was assessed via Equation (1):

$$\text{Degree of swelling (\%)} = \frac{m_t - m_0}{m_0} \quad (1)$$

where  $m_t$  (g) is the weight of the swollen sample at time  $t$ , and  $m_0$  (g) is the initial mass of the sample before swelling.

## 2.5. Batch Adsorption Experiments

### 2.5.1. pH

The pH of a solution is an important element in the protonation/deprotonation of the adsorbent's functional groups [33]. The effect of pH on the adsorption of a pharmaceutical mixture onto adsorbents in the pH range of 2–12 was examined. Initially, each pH value was modified with aqueous solutions of acid (0.1 M HCl) or base (0.1 M NaOH).

Six solutions were prepared with pH values of 2, 4, 6, 8, 10, and 12 in Erlenmeyer flasks. The solution of each pH value contained the following: 10 mg of CS-AMI and seven pharmaceutical mixtures, with each one having  $C_0 = 100 \mu\text{g/L}$  and such a quantity of HCl or NaOH to allow the final volume of the solution to be  $V = 10 \text{ mL}$ . The six flasks

were transferred to a shaking incubator with medium stirring ( $N = 125$  rpm), and the temperature was monitored at  $T = 25$  °C. The flasks remained in the incubator for 24 h. The same method was applied for CS and CS-PEI. All experiments were carried thrice. The removal efficiency ( $R$ , %) and the adsorption capacity ( $Q_t$ ) were calculated as follows:

$$Q_t = \frac{(C_0 - C_t)V}{m} \quad (2)$$

$$R = \frac{(C_0 - C_t)}{C_0} \times 100\% \quad (3)$$

where  $Q_t$  is the adsorption capacity at  $t$  ( $\mu\text{g/g}$ ),  $R$  is the removal efficiency (%),  $m$  is the weight of the adsorbent (mg), and  $C_0$  and  $C_t$  are the initial and transient concentrations ( $\mu\text{g/L}$ ).

### 2.5.2. Kinetics

The adsorption of a mixture of these pharmaceuticals was conducted by introducing 10 mg of CS-AMI into a 10 mL solution of 7 pharmaceuticals at the same concentration (100 ppb) at pH 4. The samples were taken after 5, 10, 15, 20, 30, 45, 60, 90, and 120 min. The same procedure was followed for CS and CS-PEI and was repeated 3 times. Several models have been proposed to characterise adsorption dynamics as a function of the contact time. Given their ease of use and the fact that homogeneity and equilibrium criteria are taken into consideration beforehand, the pseudo-first-order (PFO) and pseudo-second-order (PSO) are widely utilised in the field [34,35]. The equation for each model is given by Equations (4) and (5), respectively, as follows:

$$Q_t = Q_e \left(1 - e^{-k_1 t}\right) \quad (4)$$

$$Q_t = Q_e \left(1 - \frac{1}{1 + k_2 Q_e t}\right) \quad (5)$$

where  $Q_e$  is the amount of adsorbent at equilibrium ( $\mu\text{g/g}$ ),  $Q_t$  is the amount of adsorbent at time  $t$  ( $\mu\text{g/g}$ ),  $k_1$  is the pseudo-first-order rate constant (1/min), and  $k_2$  is the pseudo-second-order rate constant ( $\text{g}/(\mu\text{g}\cdot\text{min})$ ).

### 2.5.3. Effect of Mass

The adsorption experiment for the effect of the adsorbent's mass was carried out under the following conditions to determine the influence of the initial adsorbent quantity on equilibrium: In Erlenmeyer flasks, 10 solutions with the pharmaceutical mixture, with each one having  $C_0 = 100$  ppb, were prepared. Each flask's solution included 10, 20, 30, 40, 50, 60, 70, 80, 90, and 100 mg of CS-AMI, respectively, and 0.1 M HCl was the volume of each solution to achieve a pH of 4.  $V = 10$  mL. The ten flasks were placed in a shaking incubator with medium stirring ( $N = 125$  rpm) for 24 h, and  $T = 25$  °C was used. The process was repeated 2 more times. The same procedure was followed for CS and CS-PEI.

### 2.6. Analysis

For the quantitative analysis of pharmaceuticals, a Shimadzu LC-MS system (Shimadzu Corp., Tokyo, Japan) equipped with an ESI ionisation source operating in positive ionisation mode (PI) was employed. For chromatographic separation, an Athena C18 (4.6 mm  $\times$  250 mm  $\times$  5 mm particle size; CNW Technologies, Duesseldorf, Germany) column was used, and the detector voltage was set at 1.65 kV. The mobile phase was a mixture of water–0.1% formic acid (A) and methanol (B) with gradient elution at a flow rate of 0.4 mL  $\text{min}^{-1}$  at 40 °C. The drying gas was operated at a flow rate of 10 L/min at 200 °C. The nebulising pressure was 100 psi, the capillary voltage was 4500 V, and the

fragmentation voltage was set at 5 V. For each compound, the precursor molecular ion in the selected-ion monitoring (SIM) mode was acquired.

### 3. Results

#### 3.1. Characterisation Techniques

The FTIR spectra of the three composites are displayed in Figure 1. The broad peaks at  $\sim 3300\text{ cm}^{-1}$  correspond to the  $-\text{OH}$ , which exist both in chitosan and poly-acrylamide. For CS-AMI, the peak can also be induced by an overlap of chitosan N-H vibrations and  $\text{NH}_2$  from acrylamide [36]. Also, chitosan gives the vibrations at  $1665$  and  $1566\text{ cm}^{-1}$ , which are related to the carbonyl bonds of amide II and the vibrations of amide I, respectively [37]. Furthermore, the peak of C-N absorption at  $1415\text{ cm}^{-1}$  indicates the formation of chitosan-acrylamide copolymers [38]. The peaks at  $2937$  and  $2878\text{ cm}^{-1}$  are attributed to the symmetric and asymmetric C-H stretching vibrations [39]. Lastly, the high-intensity peak at  $1120\text{ cm}^{-1}$  can be explained by the saccharine structure [40].

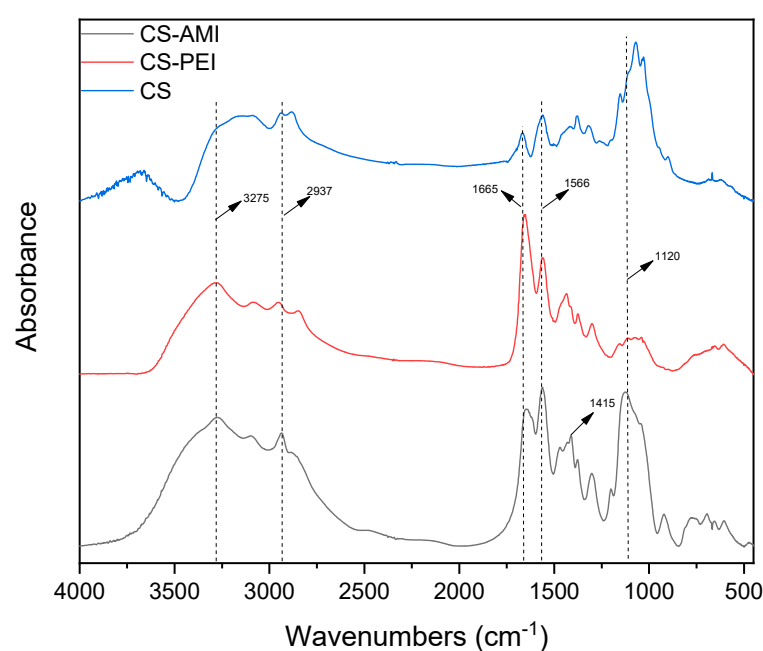
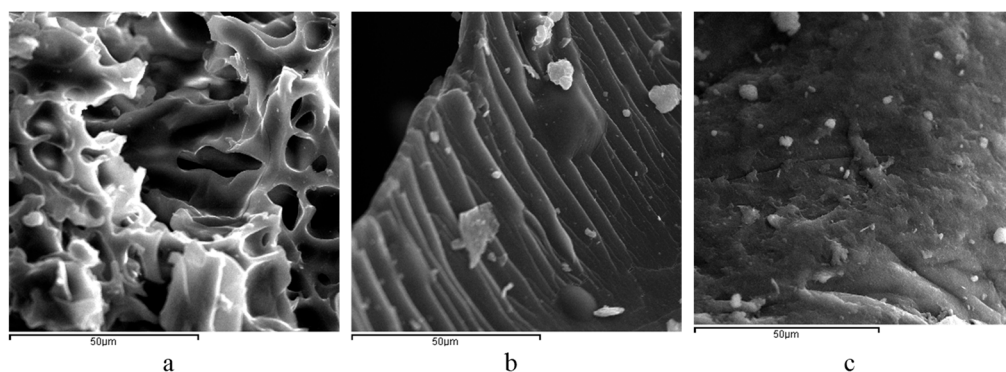


Figure 1. FTIR of adsorbents.

CS-PEI exhibits a similar structure and peaks with CS and CS-AMI. However, it presents the most intense peaks of the two amino groups out of all composites. Moreover, the peak at  $1120$  almost completely disappeared, which is the peak responsible for the asymmetric stretching of the C-O-C bridge and the skeletal vibrations involving C-O stretching, which are characteristic of the chitosan polysaccharide structure. All of the above confirm the successful synthesis of the composites.

In Figure 2, the SEM micrographs of the adsorbents can be seen in order to observe the modification of PEI and AMI on chitosan. Chitosan is a non-porous material, which is confirmed by Figure 2c indicating a tight and dense surface with a little roughness. In contrast, CS-PEI is full of scattered and well-distributed pores, as confirmed by similar research [41]. The CS-AMI derivative exhibits a more porous network with wrinkles and more homogeneity when compared to neat chitosan. This effect comes from the grafting of chitosan with acrylamide [38].



**Figure 2.** SEM images of (a) CS-PEI, (b) CS-AMI, and (c) CS.

As shown in Figure 3, the characteristic peaks of chitosan were identified at 7.4 and 19.72°, indicating its crystallinity [10]. When compared to the CS, the diffraction peak intensity of the composites at 19.72° became low. This might be because the cross-linking process reduces the consistency of the chitosan network, leading to a loss in crystallinity [42].

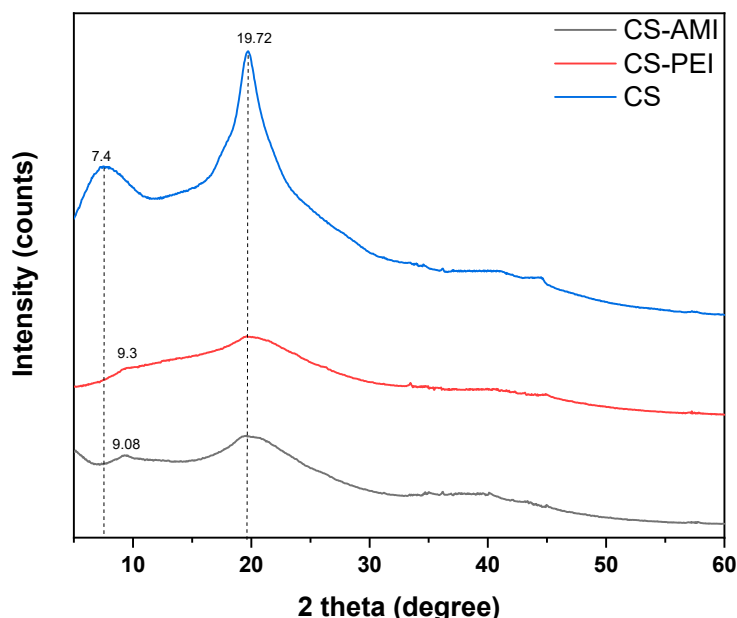


**Figure 3.** XRD patterns of chitosan derivatives.

### 3.2. Effect of pH—Adsorption Mechanism

The efficiency of removing the pollutants from the mixture at a different pH is shown in Figures 4–6. The optimum pH range was found to be 4–6, but overall better results were exhibited at pH 4, which was chosen for the rest of the experiments. The latter can be further explained by the pKa results in Table 1. In general, when the pH of the solution is lower than the pKa, adsorbates become positively charged, while when the pH > pKa, the adsorbates are in anionic form. For amphoteric compounds, when  $pK_{a1} < pH < pK_{a2}$ , they remain neutral [43]. The majority of pharmaceuticals in the mixture exist in cationic form, except for adefovir, which is neutral, and metronidazole, which is negatively charged.

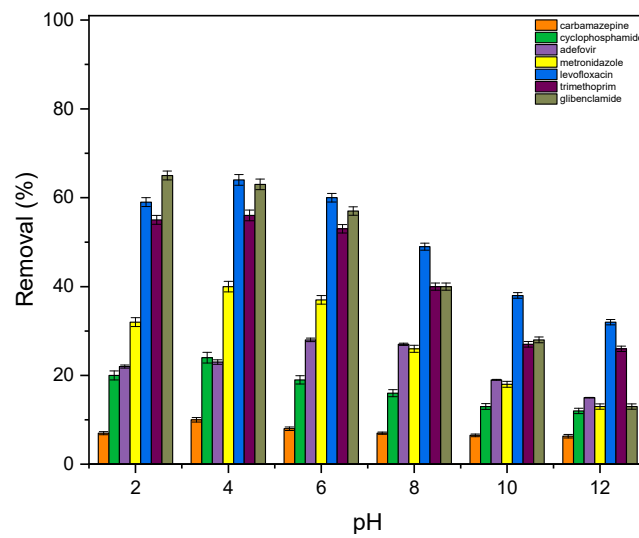


Figure 4. Effect of pH on adsorption onto CS.

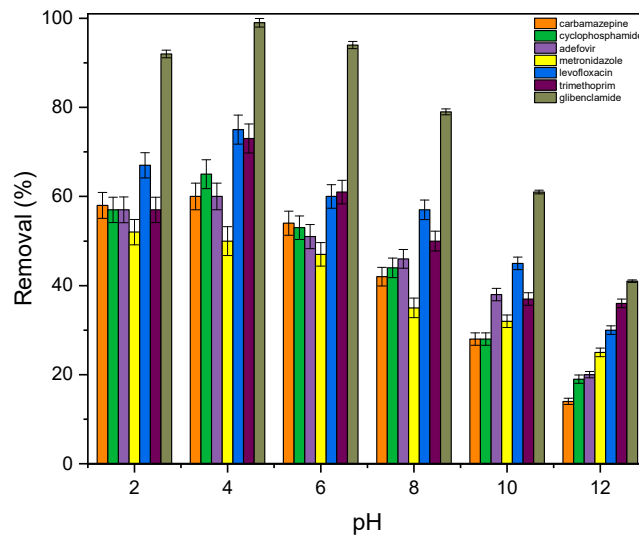


Figure 5. Effect of pH on adsorption onto CS-PEI.

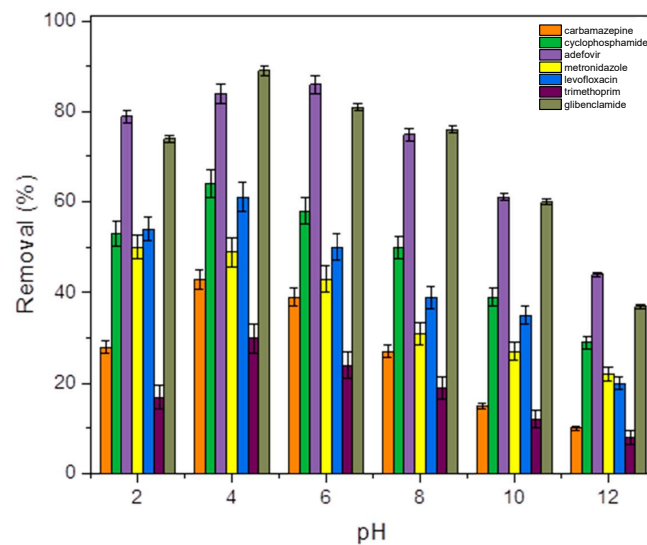


Figure 6. Effect of pH on adsorption onto CS-AMI.

Both CS-AMI and CS-PEI are modified with the addition of cationic groups (Figure S1). At these extremely acidic conditions, they are protonated ( $\text{NH}_3^+$  and  $\text{NH}_2^+$ ) due to the excess of  $\text{H}^+$  in the solution. The mechanism of adsorption for metronidazole involves electrostatic attraction between its negatively charged units, which are the hydroxyl units, and the cationic surface of the adsorbents [6,44]. As the pH increased, the electrostatic attraction eventually faded. Because the pollutants were mostly found as anions in the alkaline conditions, the electrostatic repulsion between composites and pharmaceuticals rose, severely inhibiting adsorption [45,46]. Adefovir, being neutral, develops dipole–dipole and hydrogen bonds due to  $-\text{NH}_2$  or oxygen groups [47]. CS-AMI exhibits the best removal because grafted carboxyl groups increase the hydrogen bonds between the sorbent and sorbate [48]. For cyclophosphamide and levofloxacin, there is electrostatic attraction between their chloro-groups ( $\text{Cl}^-$ ) and fluoro-groups ( $\text{F}^-$ ), respectively, and protonated amino groups ( $\text{NH}_3^+$  and  $\text{NH}_2^+$ ) of adsorbents [49]. The remaining pharmaceuticals exist in cationic form, meaning that there are repulsive forces among them, as well as with the adsorbents. So, the driving force for adsorption is hydrogen bonds [50,51]. Surprisingly, the highest removal is observed for glibenclamide.

### 3.3. Adsorption Kinetics

The pharmaceutical adsorption results as a function of the contact time for CS-PEI, CS, and CS-AMI are depicted in Figures 7–9, respectively. The processes of adsorbing the pharmaceuticals were verified by the pseudo-first-order kinetic model (PFO) and pseudo-second-order kinetic model (PSO). In each of these figures, the fitting of the best suited model is displayed. The kinetic adsorption constants of the two kinetic models are listed in Tables 2–4 for CS-PEI, CS, and CS-AMI, respectively. Adsorption occurred rapidly in the first 5 min for each compound and then progressively met equilibrium since all active sites are occupied after 25 min.

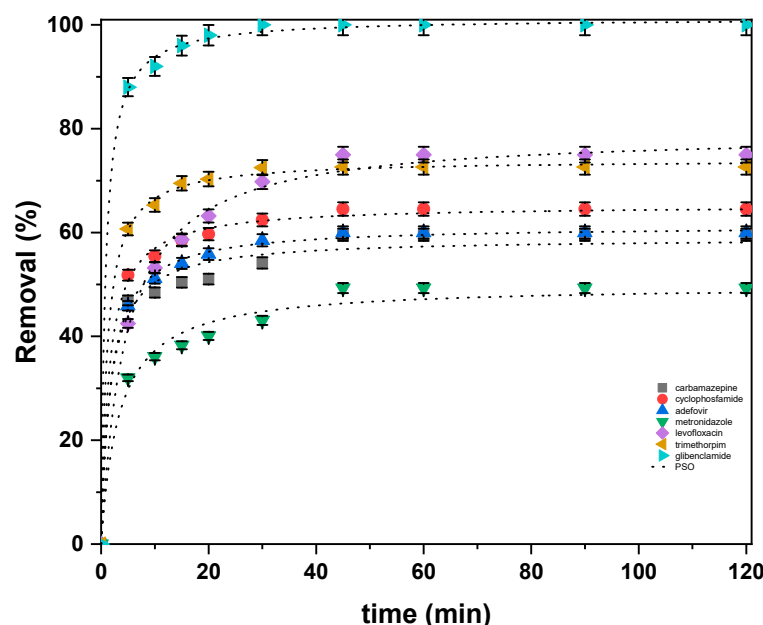


Figure 7. Effect of contact time of CS-PEI.

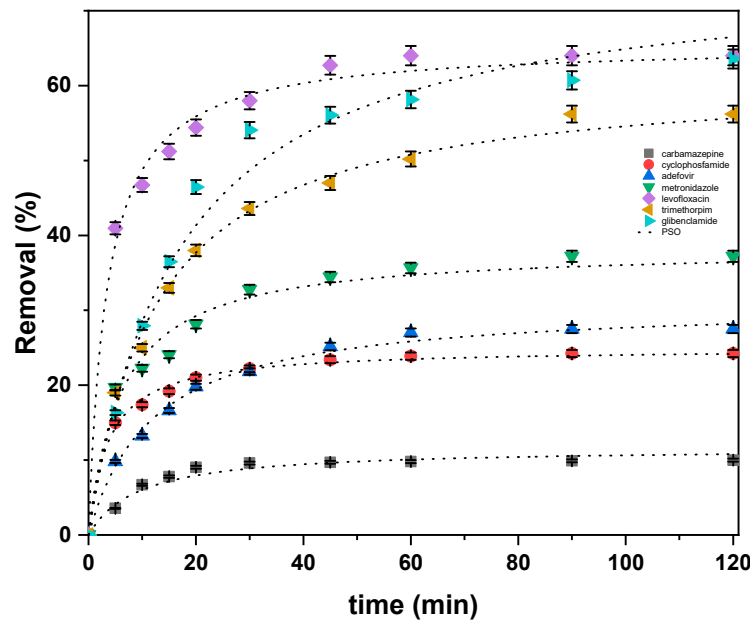


Figure 8. Effect of contact time of CS.

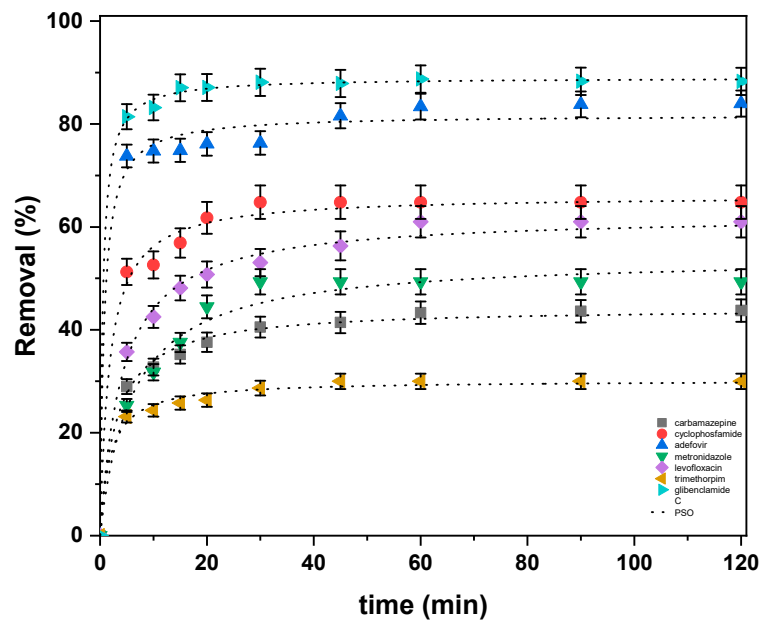


Figure 9. Effect of contact time of CS-AMI.

Table 2. Kinetic parameters for adsorption on CS-PEI.

Pharmaceutical	$k_1$ (min <sup>-1</sup> )	PFO	
			$R^2$ (-)
carbamazepine	0.330		0.950
cyclophosphamide	0.32		0.984
adefovir	0.284		0.986
metronidazole	0.195		0.900
levofloxacin	0.150		0.977
trimethoprim	0.357		0.995
glibenclamide	0.426		0.997

Table 2. Cont.

	$k_2$ ( $\mu\text{g}^{-1}\text{min}^{-1}$ )	PSO	$R^2$ (-)
carbamazepine	0.010		0.983
cyclophosphamide	0.010		0.997
adefovir	0.009		0.998
metronidazole	0.005		0.974
levofloxacin	0.002		0.996
trimethoprim	0.012		0.999
glibenclamide	0.012		0.999

Table 3. Kinetic parameters for adsorption on CS.

Pharmaceutical	$k_1$ ( $\text{min}^{-1}$ )	PFO	$R^2$ (-)
carbamazepine	0.096		0.986
cyclophosphamide	0.175		0.895
adefovir	0.075		0.959
metronidazole	0.096		0.950
levofloxacin	0.162		0.962
trimethoprim	0.062		0.980
glibenclamide	0.062		0.995

	$k_2$ ( $\mu\text{g}^{-1}\text{min}^{-1}$ )	PSO	$R^2$ (-)
carbamazepine	0.009		0.949
cyclophosphamide	0.010		0.984
adefovir	0.002		0.988
metronidazole	0.004		0.994
levofloxacin	0.004		0.993
trimethoprim	0.001		0.989
glibenclamide	0.001		0.986

Table 4. Kinetic parameters for adsorption on CS-AMI.

Pharmaceutical	$k_1$ ( $\text{min}^{-1}$ )	PFO	$R^2$ (-)
carbamazepine	0.205		0.981
cyclophosphamide	0.288		0.991
adefovir	0.515		0.996
metronidazole	0.121		0.988
levofloxacin	0.166		0.985
trimethoprim	0.293		0.972
glibenclamide	0.518		0.999

	$k_2$ ( $\mu\text{g}^{-1}\text{min}^{-1}$ )	PSO	$R^2$ (-)
carbamazepine	0.007		0.996
cyclophosphamide	0.008		0.997
adefovir	0.016		0.998
metronidazole	0.003		0.993
levofloxacin	0.003		0.997
trimethoprim	0.017		0.992
glibenclamide	0.022		0.999

Based on the results, the correlation coefficients are very close to each other, but overall, the PSO exhibits the highest values for all three adsorbents. This explains that the PSO models fits better, meaning that the adsorption process is mainly chemisorption, along with physisorption [52]. The functional groups of the materials provide chemical sorption, while the porous matrix that was observed by SEM is responsible for physical adsorption. Therefore, the adsorption mechanism can be manipulated by the surface properties of the adsorbents and drug residues, as well as the environmental conditions during the process [53].

### 3.4. Effect of Mass

In Figures 10–12, it was observed that by increasing the adsorbent dose, the removal efficiency gradually increased. However, the increase in the adsorption efficiency of high-adsorption-capacity pharmaceuticals was smaller than that of those with low capacity. In Figure 10, it is evident that by increasing the CS mass from 20 mg to 30 mg, there was little or no increase in the adsorption percentages, except from glibenclamide, where the rise from 20 mg to 30 mg exhibited an increase of ~31%. A significant rise of 45% was also observed for cyclophosphamide from 20 mg to 30mg, while metronidazole and adefovir exhibited rises of ~20% and ~24%, respectively, in the same case. The CS-PEI chart shows that the adsorbent mass does not play a significant role after the barrier of 20 mg. In contrast, for CS-AMI (Figure 12), the adsorbent dose seems to be an important parameter in the adsorption of pollutants. It is possible that the process relies more on chemisorption, and the increase in CS-AMI in the solution comes with an increase in active sites. The existence of pharmaceuticals in wastewaters are in ppb ( $\mu\text{g/L}$ ) or, in some extreme conditions, in ppm (mg/L). To further simulate real conditions, the simultaneous removal in mixtures was investigated, but not the single components. The obtained results indicate that the adsorbents are able to perform well in such conditions and can eliminate a considerable amount of pollutants.

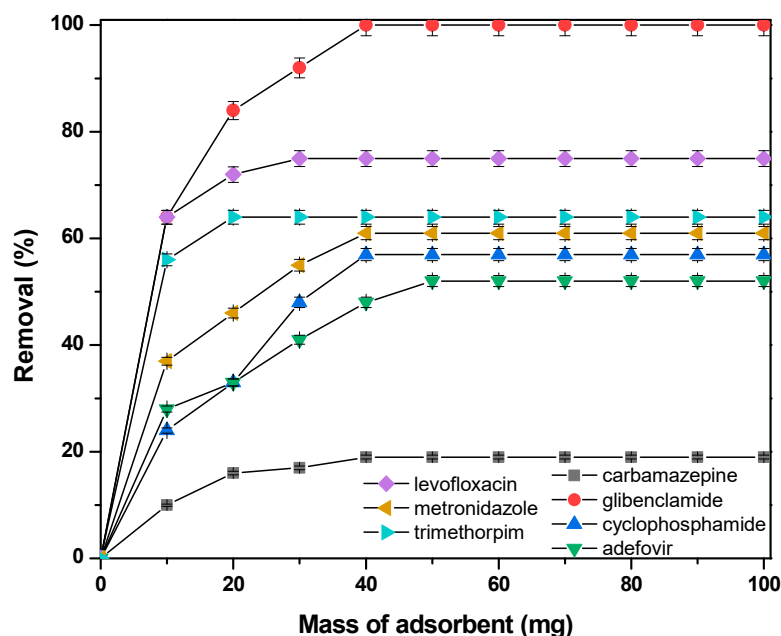


Figure 10. Effect of CS mass on equilibrium.

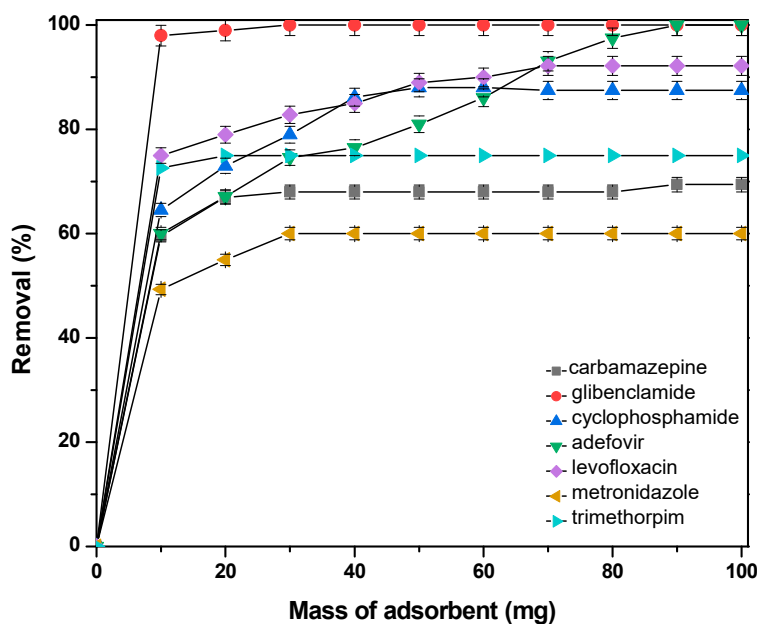


Figure 11. Effect of CS-PEI mass on equilibrium.

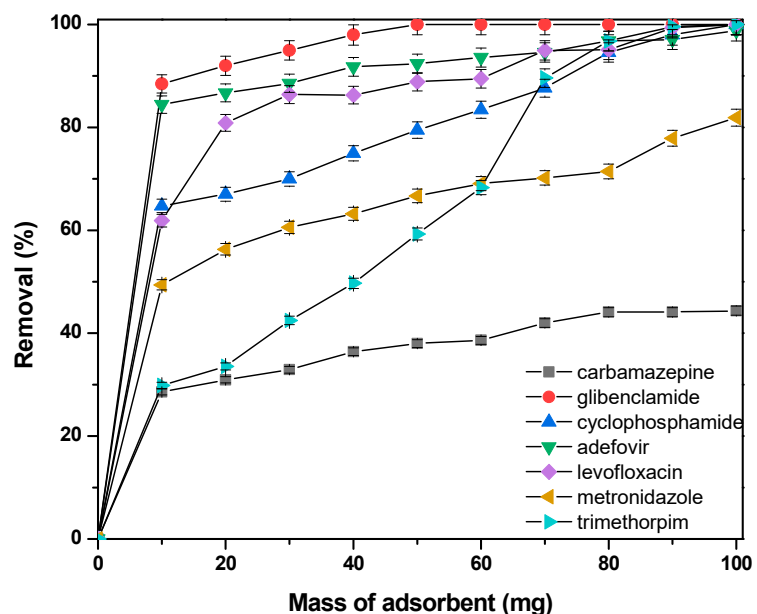


Figure 12. Effect of CS-AMI mass on equilibrium.

#### 4. Conclusions

The present research seeks to gain an understanding of pharmaceutical adsorption onto CS derivatives and to assess the impacts of essential parameters on adsorption efficiency. The findings indicate that CS, CS-PEI, and CS-AMI are effective materials for removing pharmaceuticals from water solutions; however, the modified materials appear to be more efficient. The kinetic studies revealed that the PSO kinetic model presented better fitting than the PFO model for all three materials, showing that the main mechanisms are chemical adsorption and electrostatic interactions. Moreover, adsorption on CS, CS-PEI, and CS-AMI appeared to be considerably influenced by the solution’s pH and pharmaceutical features, such as molecular charge (neutral, anionic, and cationic). The optimum pH range was found to be 4–6, but overall better results were obtained at pH 4. Finally, variations in the adsorbate quantity had no significant effect on the medicinal

adsorption efficiency. As a result, manufactured adsorbents offer an exciting promise for future pharmaceutical wastewater treatment.

**Supplementary Materials:** The following supporting information can be downloaded at: <https://www.mdpi.com/article/10.3390/macromol4020018/s1>. Figure S1: Chemical structure of (a) CS-AMI and (b) CS-PEI.

**Author Contributions:** M.P.: Formal Analysis, Investigation, Validation, and Software; K.N.M.: Methodology, Formal Analysis, Visualisation, Validation, and Writing—Original Draft Preparation; E.E.: Validation, Visualisation, Writing—Original Draft Preparation, Reviewing, and Editing; D.N.B.: Formal Analysis, Visualisation, Validation, and Reviewing; G.Z.K.: Conceptualisation, Methodology, Validation, Visualisation, Writing—Original Draft Preparation, Reviewing, and Editing; D.A.L.: Conceptualisation, Methodology, Validation, Reviewing, Editing, and Supervision. All authors have read and agreed to the published version of the manuscript.

**Funding:** This research received no external funding.

**Data Availability Statement:** The data presented in this study are available on request from the corresponding author.

**Conflicts of Interest:** The authors declare no conflicts of interest.

## References

1. Abd El-Monaem, E.M.; Eltaweil, A.S.; Elshishini, H.M.; Hosny, M.; Abou Alsoaud, M.M.; Attia, N.F.; El-Subruiti, G.M.; Omer, A.M. Sustainable Adsorptive Removal of Antibiotic Residues by Chitosan Composites: An Insight into Current Developments and Future Recommendations. *Arab. J. Chem.* **2022**, *15*, 103743. [[CrossRef](#)] [[PubMed](#)]
2. Gkika, D.A.; Mitropoulos, A.C.; Kokkinos, P.; Lambropoulou, D.A.; Kalavrouziotis, I.K.; Bikiaris, D.N.; Kyzas, G.Z. Modified Chitosan Adsorbents in Pharmaceutical Simulated Wastewaters: A Review of the Last Updates. *Carbohydr. Polym. Technol. Appl.* **2023**, *5*, 100313. [[CrossRef](#)]
3. Bhuyan, A.; Ahmaruzzaman, M. Recent Advances in New Generation Nanocomposite Materials for Adsorption of Pharmaceuticals from Aqueous Environment. *Environ. Sci. Pollut. Res.* **2023**, *30*, 39377–39417. [[CrossRef](#)] [[PubMed](#)]
4. McDougall, L.; Thomson, L.; Brand, S.; Wagstaff, A.; Lawton, L.A.; Petrie, B. Adsorption of a Diverse Range of Pharmaceuticals to Polyethylene Microplastics in Wastewater and Their Desorption in Environmental Matrices. *Sci. Total Environ.* **2022**, *808*, 152071. [[CrossRef](#)] [[PubMed](#)]
5. Al-Jubouri, S.M.; Al-Jendeel, H.A.; Rashid, S.A.; Al-Batty, S. Antibiotics Adsorption from Contaminated Water by Composites of ZSM-5 Zeolite Nanocrystals Coated Carbon. *J. Water Process Eng.* **2022**, *47*, 102745. [[CrossRef](#)]
6. Bai, H.; Zhang, Q.; Zhou, X.; Chen, J.; Chen, Z.; Liu, Z.; Yan, J.; Wang, J. Removal of Fluoroquinolone Antibiotics by Adsorption of Dopamine-Modified Biochar Aerogel. *Korean J. Chem. Eng.* **2023**, *40*, 215–222. [[CrossRef](#)]
7. Agustin, M.B.; Mikkonen, K.S.; Kemell, M.; Lahtinen, P.; Lehtonen, M. Systematic Investigation of the Adsorption Potential of Lignin- and Cellulose-Based Nanomaterials towards Pharmaceuticals. *Environ. Sci. Nano* **2022**, *9*, 2006–2019. [[CrossRef](#)]
8. Okolie, J.A.; Savage, S.; Ogbaga, C.C.; Gunes, B. Assessing the Potential of Machine Learning Methods to Study the Removal of Pharmaceuticals from Wastewater Using Biochar or Activated Carbon. *Total Environ. Res. Themes* **2022**, *1–2*, 100001. [[CrossRef](#)]
9. Ferrah, N.; Merghache, D.; Meftah, S.; Benbellil, S. A New Alternative of a Green Polymeric Matrix Chitosan/Alginate-Polyethylenimine-methylene Phosphonic Acid for Pharmaceutical Residues Adsorption. *Environ. Sci. Pollut. Res.* **2022**, *29*, 13675–13687. [[CrossRef](#)]
10. Mashile, P.P.; Nomngongo, P.N. Magnetic Cellulose-Chitosan Nanocomposite for Simultaneous Removal of Emerging Contaminants: Adsorption Kinetics and Equilibrium Studies. *Gels* **2021**, *7*, 190. [[CrossRef](#)]
11. Ahmed, M.; Mavukkandy, M.O.; Giwa, A.; Elektorowicz, M.; Katsou, E.; Khelifi, O.; Naddeo, V.; Hasan, S.W. Recent Developments in Hazardous Pollutants Removal from Wastewater and Water Reuse within a Circular Economy. *NPJ Clean Water* **2022**, *5*, 12. [[CrossRef](#)]
12. Bhatt, P.; Joshi, S.; Urper Bayram, G.M.; Khati, P.; Simsek, H. Developments and Application of Chitosan-Based Adsorbents for Wastewater Treatments. *Environ. Res.* **2023**, *226*, 115530. [[CrossRef](#)] [[PubMed](#)]
13. Kumar, A.; Patra, C.; Rajendran, H.K.; Narayanasamy, S. Activated Carbon-Chitosan Based Adsorbent for the Efficient Removal of the Emerging Contaminant Diclofenac: Synthesis, Characterization and Phytotoxicity Studies. *Chemosphere* **2022**, *307*, 135806. [[CrossRef](#)] [[PubMed](#)]
14. Khan, M.; Ali, S.W.; Shahadat, M.; Sagadevan, S. Applications of Polyaniline-Impregnated Silica Gel-Based Nanocomposites in Wastewater Treatment as an Efficient Adsorbent of Some Important Organic Dyes. *Green Process. Synth.* **2022**, *11*, 617–630. [[CrossRef](#)]
15. Ganthavee, V.; Trzcinski, A.P. Removal of Pharmaceutically Active Compounds from Wastewater Using Adsorption Coupled with Electrochemical Oxidation Technology: A Critical Review. *J. Ind. Eng. Chem.* **2023**, *126*, 20–35. [[CrossRef](#)]

16. Nordin, A.H.; Ngadi, N.; Ilyas, R.A.; Abd Latif, N.A.F.; Nordin, M.L.; Mohd Syukri, M.S.; Nabgan, W.; Paiman, S.H. Green Surface Functionalization of Chitosan with Spent Tea Waste Extract for the Development of an Efficient Adsorbent for Aspirin Removal. *Environ. Sci. Pollut. Res.* **2023**, *30*, 125048–125065. [[CrossRef](#)] [[PubMed](#)]
17. Chan, K.; Morikawa, K.; Shibata, N.; Zinchenko, A. Adsorptive Removal of Heavy Metal Ions, Organic Dyes, and Pharmaceuticals by DNA–Chitosan Hydrogels. *Gels* **2021**, *7*, 112. [[CrossRef](#)] [[PubMed](#)]
18. Zhao, X.; Wang, X.; Lou, T. Simultaneous Adsorption for Cationic and Anionic Dyes Using Chitosan/Electrospun Sodium Alginate Nanofiber Composite Sponges. *Carbohydr. Polym.* **2022**, *276*, 118728. [[CrossRef](#)] [[PubMed](#)]
19. Saheed, I.O.; Oh, W.D.; Suah, F.B.M. Chitosan Modifications for Adsorption of Pollutants—A Review. *J. Hazard. Mater.* **2021**, *408*, 124889. [[CrossRef](#)]
20. Kyzas, G.Z.; Siafaka, P.I.; Lambropoulou, D.A.; Lazaridis, N.K.; Bikiaris, D.N. Poly(Itaconic Acid)-Grafted Chitosan Adsorbents with Different Cross-Linking for Pb(II) and Cd(II) Uptake. *Langmuir* **2014**, *30*, 120–131. [[CrossRef](#)]
21. Alkabli, J. Progress in Preparation of Thiolated, Crosslinked, and Imino-Chitosan Derivatives Targeting Specific Applications. *Eur. Polym. J.* **2022**, *165*, 110998. [[CrossRef](#)]
22. Torkaman, S.; Rahmani, H.; Ashori, A.; Najafi, S.H.M. Modification of Chitosan Using Amino Acids for Wound Healing Purposes: A Review. *Carbohydr. Polym.* **2021**, *258*, 117675. [[CrossRef](#)] [[PubMed](#)]
23. Mansouri, H.; Carmona, R.J.; Gomis-Berenguer, A.; Souissi-Najar, S.; Ouederni, A.; Ania, C.O. Competitive Adsorption of Ibuprofen and Amoxicillin Mixtures from Aqueous Solution on Activated Carbons. *J. Colloid. Interface Sci.* **2015**, *449*, 252–260. [[CrossRef](#)] [[PubMed](#)]
24. Brugnerotto, J.; Lizardi, J.; Goycoolea, F.M.; Argüelles-Monal, W.; Desbrières, J.; Rinaudo, M. An Infrared Investigation in Relation with Chitin and Chitosan Characterization. *Polymer* **2001**, *42*, 3569–3580. [[CrossRef](#)]
25. Rinaudo, M. Chitin and Chitosan: Properties and Applications. *Prog. Polym. Sci.* **2006**, *31*, 603–632. [[CrossRef](#)]
26. Chatterjee, S.; Chatterjee, T.; Woo, S.H. Influence of the Polyethyleneimine Grafting on the Adsorption Capacity of Chitosan Beads for Reactive Black 5 from Aqueous Solutions. *Chem. Eng. J.* **2011**, *166*, 168–175. [[CrossRef](#)]
27. Zhou, L.; Jin, J.; Liu, Z.; Liang, X.; Shang, C. Adsorption of Acid Dyes from Aqueous Solutions by the Ethylenediamine-Modified Magnetic Chitosan Nanoparticles. *J. Hazard. Mater.* **2011**, *185*, 1045–1052. [[CrossRef](#)]
28. Al-Odaini, N.A.; Zakaria, M.P.; Yaziz, M.I.; Surif, S.; Abdulghani, M. The Occurrence of Human Pharmaceuticals in Wastewater Effluents and Surface Water of Langat River and Its Tributaries, Malaysia. *Int. J. Environ. Anal. Chem.* **2013**, *93*, 245–264. [[CrossRef](#)]
29. Gworek, B.; Kijeńska, M.; Zaborowska, M.; Wrzosek, J.; Tokarz, L.; Chmielewski, J. Occurrence of Pharmaceuticals in Aquatic Environment—A Review. *DWT* **2020**, *184*, 375–387. [[CrossRef](#)]
30. Queirós, V.; Azeiteiro, U.M.; Soares, A.M.V.M.; Freitas, R. The Antineoplastic Drugs Cyclophosphamide and Cisplatin in the Aquatic Environment—Review. *J. Hazard. Mater.* **2021**, *412*, 125028. [[CrossRef](#)]
31. Almeida, Â.; Soares, A.M.V.M.; Esteves, V.I.; Freitas, R. Occurrence of the Antiepileptic Carbamazepine in Water and Bivalves from Marine Environments: A Review. *Environ. Toxicol. Pharmacol.* **2021**, *86*, 103661. [[CrossRef](#)] [[PubMed](#)]
32. Jain, S.; Kumar, P.; Vyas, R.K.; Pandit, P.; Dalai, A.K. Occurrence and Removal of Antiviral Drugs in Environment: A Review. *Water Air Soil. Pollut.* **2013**, *224*, 1410. [[CrossRef](#)]
33. Amalina, F.; Abd Razak, A.S.; Krishnan, S.; Zularisam, A.W.; Nasrullah, M. A Review of Eco-Sustainable Techniques for the Removal of Rhodamine B Dye Utilizing Biomass Residue Adsorbents. *Phys. Chem. Earth Parts A/B/C* **2022**, *128*, 103267. [[CrossRef](#)]
34. Ho, Y.S.; Ng, J.C.Y.; McKay, G. Kinetics of Pollutant Sorption by Biosorbents: Review. *Sep. Purif. Methods* **2000**, *29*, 189–232. [[CrossRef](#)]
35. Yan, M.; Huang, W.; Li, Z. Chitosan Cross-Linked Graphene Oxide/Lignosulfonate Composite Aerogel for Enhanced Adsorption of Methylene Blue in Water. *Int. J. Biol. Macromol.* **2019**, *136*, 927–935. [[CrossRef](#)]
36. Akkaya, R.; Akkaya, B.; Çakıcı, G.T. Chitosan–Poly(Acrylamide-Co-Maleic Acid) Composite Synthesis, Characterization, and Investigation of Protein Adsorption Behavior. *Polym. Bull.* **2023**, *80*, 4153–4168. [[CrossRef](#)]
37. Maroulas, K.N.; Trikkaliotis, D.G.; Metaxa, Z.S.; AbdelAll, N.; Alodhayb, A.; Khouqeer, G.A.; Kyzas, G.Z. Super-Hydrophobic Chitosan/Graphene-Based Aerogels for Oil Absorption. *J. Mol. Liq.* **2023**, *390*, 123071. [[CrossRef](#)]
38. Desnelli, D.; Eliza, E.; Mara, A.; Rachmat, A. Synthesis of Copolymer of Chitosan with Acrylamide as an Adsorbent for Heavy Metal Waste Treatment. *IOP Conf. Ser. Mater. Sci. Eng.* **2020**, *833*, 12064. [[CrossRef](#)]
39. Soradach, S.; Kengkwasingh, P.; Williams, A.C.; Khutoryanskiy, V. V Synthesis and Evaluation of Poly(3-Hydroxypropyl Ethylene-Imine) and Its Blends with Chitosan Forming Novel Elastic Films for Delivery of Haloperidol. *Pharmaceutics* **2022**, *14*, 2671. [[CrossRef](#)]
40. Shi, A.; Dai, X.; Jing, Z. Tough and Self-Healing Chitosan/Poly(Acrylamide-Co-Acrylic Acid) Double Network Hydrogels. *Polym. Sci. Ser. A* **2020**, *62*, 228–239. [[CrossRef](#)]
41. Zhang, C.; Yang, T.; Liu, J.; Duan, Q.; Song, J.; Yin, Y.; Wang, H. Multi-Component Sorption of Pb<sup>2+</sup>, Cu<sup>2+</sup> and Ni<sup>2+</sup> on PEI Modified Chitosan-Based Hybrid Membranes. *J. Mol. Liq.* **2023**, *371*, 121091. [[CrossRef](#)]
42. Meng, J.; Cui, J.; Yu, S.; Jiang, H.; Zhong, C.; Hongshun, J. Preparation of Aminated Chitosan Microspheres by One-Pot Method and Their Adsorption Properties for Dye Wastewater. *R. Soc. Open Sci.* **2019**, *6*, 182226. [[CrossRef](#)] [[PubMed](#)]
43. Huang, K.; Yang, S.; Liu, X.; Zhu, C.; Qi, F.; Wang, K.; Wang, J.; Wang, Q.; Wang, T.; Ma, P. Adsorption of Antibiotics from Wastewater by Cabbage-Based N, P Co-Doped Mesoporous Carbon Materials. *J. Clean. Prod.* **2023**, *391*, 136174. [[CrossRef](#)]

44. Ghiasi, F.; Solaimany Nazar, A.R.; Farhadian, M.; Tangestaninejad, S.; Emami, N. Synthesis of Aqueous Media Stable MIL101-OH/Chitosan for Diphenhydramine and Metronidazole Adsorption. *Environ. Sci. Pollut. Res.* **2022**, *29*, 24286–24297. [[CrossRef](#)] [[PubMed](#)]
45. Liao, X.; Chen, C.; Liang, Z.; Zhao, Z.; Cui, F. Selective Adsorption of Antibiotics on Manganese Oxide-Loaded Biochar and Mechanism Based on Quantitative Structure–Property Relationship Model. *Bioresour. Technol.* **2023**, *367*, 128262. [[CrossRef](#)]
46. Teo, C.Y.; Jong, J.S.J.; Chan, Y.Q. Carbon-Based Materials as Effective Adsorbents for the Removal of Pharmaceutical Compounds from Aqueous Solution. *Adsorpt. Sci. Technol.* **2022**, *2022*, e3079663. [[CrossRef](#)]
47. Malesic-Eleftheriadou, N.; Trikkaliotis, D.G.; Evgenidou, E.; Kyzas, G.Z.; Bikiaris, D.N.; Lambropoulou, D.A. New Biobased Chitosan/Polyvinyl Alcohol/Graphene Oxide Derivatives for the Removal of Pharmaceutical Compounds from Aqueous Mixtures. *J. Mol. Liq.* **2023**, *387*, 122673. [[CrossRef](#)]
48. Kyzas, G.Z.; Lazaridis, N.K. Reactive and Basic Dyes Removal by Sorption onto Chitosan Derivatives. *J. Colloid. Interface Sci.* **2009**, *331*, 32–39. [[CrossRef](#)] [[PubMed](#)]
49. Malesic-Eleftheriadou, N.; Evgenidou, E.; Lazaridou, M.; Bikiaris, D.N.; Yang, X.; Kyzas, G.Z.; Lambropoulou, D.A. Simultaneous Removal of Anti-Inflammatory Pharmaceutical Compounds from an Aqueous Mixture with Adsorption onto Chitosan Zwitterionic Derivative. *Colloids Surf. A Physicochem. Eng. Asp.* **2021**, *619*, 126498. [[CrossRef](#)]
50. Nezhadali, A.; Koushali, S.E.; Divsar, F. Synthesis of Polypyrrole—Chitosan Magnetic Nanocomposite for the Removal of Carbamazepine from Wastewater: Adsorption Isotherm and Kinetic Study. *J. Environ. Chem. Eng.* **2021**, *9*, 105648. [[CrossRef](#)]
51. Suriyanon, N.; Punyapalaku, P.; Ngamcharusrivichai, C. Mechanistic Study of Diclofenac and Carbamazepine Adsorption on Functionalized Silica-Based Porous Materials. *Chem. Eng. J.* **2013**, *214*, 208–218. [[CrossRef](#)]
52. Hu, Y.; Chen, Y.; Guo, Y.; Liu, C.; Gao, Y.; Xiong, Y.; Jia, Z.; Wang, X.; Zhang, X.; Li, H.; et al. Preparation of High Flux GO/PS-DVB/PAN Membrane by Filtering Layer-by-Layer Assembly Method for Adsorption of Antibiotics from Water. *J. Inorg. Organomet. Polym.* **2023**, *33*, 2292–2304. [[CrossRef](#)]
53. Li, Z.; Jiang, H.; Wang, X.; Wang, C.; Wei, X. Effect of PH on Adsorption of Tetracycline Antibiotics on Graphene Oxide. *Int. J. Environ. Res. Public Health* **2023**, *20*, 2448. [[CrossRef](#)] [[PubMed](#)]

**Disclaimer/Publisher’s Note:** The statements, opinions and data contained in all publications are solely those of the individual author(s) and contributor(s) and not of MDPI and/or the editor(s). MDPI and/or the editor(s) disclaim responsibility for any injury to people or property resulting from any ideas, methods, instructions or products referred to in the content.